Maximum Working Volume Evaluation in a Non-Canonical Reverberation Chamber

Sergio Avila, Mario Alves dos Santos Junior, Djonny Weinzierl, Laurent Krähenbühl, Ronan Perrussel, Christian Vollaire, Carlos Sartori, Luiz Lebensztajn, José Cardoso

Maximum Working Volume Evaluation in a Non-Canonical Reverberation Chamber

S. L. Avila[1,2], M. A. Santos Jr.[1], D. Weinzierl[1,3], L. Krähenbühl[4], R. Perrussel[4], C. Vollaire[4], C. A. F. Sartori[1], L. Lebensztajn[1], and J. R. Cardoso[1]

[1]LMAG/PEA/EPUSP, 05508-900, São Paulo, SP, Brazil
[2]Fundação Centros de Referência em Tecnologias Inovadoras, 88040-970, Florianópolis, SC, Brazil
[3]Centro Universitário de Jaraguá do Sul, Rua dos Imigrantes, 89254-430, Jaraguá do Sul, SC, Brazil
[4]Laboratoire Ampère (CNRS UMR5005), Université de Lyon, Ecole Centrale de Lyon, 69134, Ecully Cedex, France

This paper presents a procedure for evaluating the performance of reverberation chambers, by approximating the maximum working volume in a given configuration. The evaluation of this volume is based on the geometrical and physical constraints, e.g., the ones related to the internal E-field distribution recommended by standards. The importance of the present work is related to the development of a non-canonical reverberation chamber configuration, whose excitation is carried out by transmission lines, instead of antennas plus paddles.

***Index Terms*—Optimization, reverberation chambers, working volume.**

I. Introduction

In recent years, the concern about the compliance of electro-electronic devices is arising, since the manufacturers are replacing the analogical and mechanical systems by digital ones, and the electromagnetic compatibility (EMC) tests are used to insure the correct performance of theses devices under normal operation conditions. One of the problems presented by EMC test environments is their cost. Alternatives, such as reverberation chambers, are becoming attractive to perform radiated immunity tests.

Presented originally by Mendes [1], a canonical reverberation chamber is an electrically large, highly conductive enclosed cavity equipped with metallic paddle wheels, which rotate independently, changing the internal dimension of the chamber. The only fields, which can exist within a chamber with perfect conducting walls, are the classical transverse electric and magnetic modes to any of its coordinate axis, $\mathrm{TE}_{\mathrm{mnp}}$ and $\mathrm{TM}_{\mathrm{mnp}}$, respectively. These correspond to the only possible solutions for the Maxwell equations, which satisfy the boundary conditions of zero tangential E-fields on the walls. When the metallic paddle wheels are introduced into the chamber, the new solution for this problem is obtained by the superposition of these modes. This particular solution satisfies the boundary conditions of the problem domain.

When the chamber is excited, over three times the fundamental frequency [2], one could find a resulting multimode electromagnetic environment that can be stirred by the mechanical tuners, making it useful to perform electromagnetic immunity measurements on electro-electronic equipments. Otherwise, the chamber mode density and the effectiveness of the mechanical tuners determine the lowest useable frequency (LUF) [2]. Whilst a range of EMC measurement techniques exist for use in the frequency range up to GHz, new measurement techniques are required below the LUF. Therefore typical reverberation chambers are operated above 200 MHz and operations below 200 MHz require chambers that are larger than typical shielded rooms, once the fundamental frequency depends inversely on the chamber dimensions.

This paper presents an investigation of non-canonical reverberation chamber configurations, originally proposed by Perini and Cohen, whose excitation is carried out through a set of wires [3]. It should be mentioned that, as wires support TEM fields, this approach allows us to excite, besides the common TE and TM modes, the TEM mode within the chamber. This widens the generated frequencies range regarding the resulting LUF.

The optimization techniques are used to search the working volumes [5], [6] that fulfill predefined requirements of field uniformity and mean electric field. This paper takes into account a predefined chamber, i.e., both the dimensions of the chamber and the position of the wires are known and will be not changed. The main target of the work is focused on the better performance of the chamber. This could be understood in two different aspects: one could use the chamber in order to test high volume objects or this object could be tested under high electric field intensity. This allows us to define two different scenarios: the first one is the determination of a particular working volume, with a prescribed electric field. The second one is associated to the behavior of the chamber: working volume improvements are associated to a decrease of the mean electric field, and vice-versa. Therefore, the search for a set of "good" working volumes will characterize the capability of the chamber to perform EMC tests on objects considering several volumes and distinct electric field intensities. For both scenarios some geometrical and physical constraints were taken into account.

II. Non-Canonical Chamber Proposition

Fig. 1 shows the analyzed chamber, which is excited by three wires [5]. The dimensions of the chamber are: $4.6 \times 2.7 \times 5.2$ m. The wires 1, 2, and 3 are placed along the x, y and z axes, at: $y_1 = 4.1$ m, $z_1 = 2.2$ m; $x_2 = 0.5$ m, $z_2 = 2.4$ m, and $x_3 = 0.7$ m, $y_3 = 3.9$ m, respectively. The first resonance frequency of the chamber yields approximately 43.5 MHz. In order to have at least 100 propagating modes within the chamber the operation frequency should be higher than 130 MHz.

Manuscript received October 07, 2008. Current version published February 19, 2009. Corresponding author: L. Lebensztajn (e-mail: leb@pea.usp.br).

Color versions of one or more of the figures in this paper are available online at http://ieeexplore.ieee.org.

Digital Object Identifier 10.1109/TMAG.2009.2012766

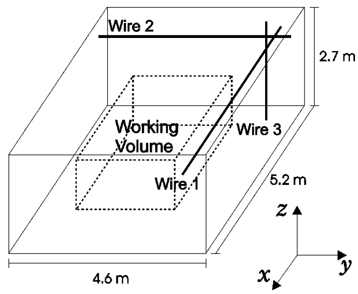

Fig. 1. Chamber configuration excited by three wires.

Simulations were performed using the finite integration technique (FIT), with fixed positions for wires 1, 2, and 3, and results are exported to a file, which was read by our optimization environment, and where the optimization algorithm is performed. Since the FIT is a well known technique and its descriptions and details have already been presented in several publications, they are not described in this paper [4].

The walls of the chamber and the wires were modelled as perfect electric conductors (PEC). Each wire is fed by an independent excitation port and terminated with a 270 Ω load at its end. The simulations considered an input power of 1 W at each wire and an excitation frequency of 10 MHz, which corresponds to a value approximately four times lower than the lowest resonance frequency of the chamber shown in Fig. 1.

III. Statistical Analysis Description

In order to verify the electric field distribution within the reverberation chamber, a preselected configuration was implemented and analyzed based on numerical simulations. For this purpose, the standard deviation values are calculated based on the individual and combined arithmetic per-axis means, as given by

$$\bar{E}_k = \frac{1}{N}\sum_{i=1}^{N} E_{k,i} \tag{1}$$

$$\bar{E}_{x,y,z} = \frac{1}{3N}\sum_{k=\{x,y,z\}}\sum_{i=1}^{N} E_{k,i} \tag{2}$$

where $\bar{E}_k$ is the arithmetic mean of the k-component of the maximum electric field E_k, $\bar{E}_{x,y,z}$ the arithmetic mean of the electric field considering the three single components, and N the number of the obtained samples. The magnitude of the k-component of the electric field is defined as the square root of the sum of the squares of its real and imaginary parts

$$|E_k| = \sqrt{(\mathrm{Re}\{E_k\})^2 + (\mathrm{Im}\{E_k\})^2}. \tag{3}$$

Based on the presented equations, the individual σ_k and combined $\sigma_{x,y,z}$ standard deviation values are [2]

$$\sigma_k = \sqrt{\sum_{i=1}^{N}(|E_{k,i}| - \bar{E}_k)^2/(N-1)} \tag{4}$$

$$\sigma_{x,y,z} = \sqrt{\sum_{k=\{x,y,z\}}\sum_{i=1}^{N}(|E_{k,i}| - \bar{E}_{x,y,z})^2/(3N-1)} \tag{5}$$

or, in decibel notation

$$\hat{\sigma}_k = 20\log_{10}[(\sigma_k + \bar{E}_k)/\bar{E}_k] \tag{6}$$

$$\hat{\sigma}_{x,y,z} = 20\log_{10}\frac{\sigma_{x,y,z} + \bar{E}_{x,y,z}}{\bar{E}_{x,y,z}}. \tag{7}$$

In compliance with [2], both the individual and combined standard deviation values considering sufficient statistical field uniformity and a given uncertainty within the frequency range of 80 MHz to 1 GHz should satisfy the following conditions: 4 dB in the range from 80 MHz until 100 MHz, decreasing linearly to 3 dB at 400 MHz, and 3 dB from 400 MHz up to 1 GHz. Values below 80 MHz are not considered by this standard.

IV. Optimization Techniques and the Working Volume

A working volume is assumed to be a region inside the reverberation chamber where the homogeneity of the electric field attains a prescribed level. EMC tests could be performed if this minimum homogeneity level is achieved, and the mean value within the working volume should be as high as possible considering low input power.

Regarding the working volume of a certain reverberation chamber, there are at least two scenarios to be analyzed. The first one concerns the search for a maximum working volume, taking into account an electric field threshold and a minimum homogeneity level. The second scenario deals with the characterization of the reverberation chamber. The maximum volume depends upon the mean electric field, i.e., the problem yields the maximization of the working volume and the electric field constrained to the homogeneity level of the electric field. When the working volume increases the electric field decreases and vice-versa; so a multiobjective optimization algorithm should be employed.

In the first scenario we are interested in a particular working volume, where the equipment under test (EUT) could be placed. This volume has the following attributes: its position in the chamber, its volume and the mean value of the electric field. The main attribute of this volume concerns the best volume to test the equipment in predefined electric field value and homogeneity. In the second scenario, the main interest is the reverberation chamber characterization, which is associated to a set of working volumes. In this set, inside of some working volume the electric field is high, whereas the volume is low. There are other working volumes, which belong to this set, but have low electric field and high volume. Inside the working volumes the field homogeneity is constrained by predefined values. When the chamber characterization is performed, the engineer could make a choice to obtain the most suitable volume to perform the electromagnetic immunity test.

A. Determination of the Working Volume

In order to obtain the working volume considering a prescribed value of mean electric field, the value of the combined electric field, as defined by (2), will be adopted as the mean value. The problem consists in finding the solution to the constrained optimization problem as follows, where $\mathrm{E_{presc.}}$ is the prescribed value of the combined field inside the working volume

$$\begin{array}{rl} \text{Max} & (\text{Working Volume}) \\ \text{Submitted to} & \begin{cases} \bar{\mathrm{E}}_{\mathrm{x,y,z}} = \mathrm{E_{presc.}} \\ \mathrm{Max}(\hat{\sigma}_{\mathrm{x}}, \hat{\sigma}_{\mathrm{y}}, \hat{\sigma}_{\mathrm{z}}, \hat{\sigma}_{\mathrm{x,y,z}}) \le 4\ \text{dB}. \end{cases} \end{array} \tag{8}$$

In order to solve it, the optimization problem was rewritten as an unconstrained optimization problem, where both the equality and inequality constraints were treated as penalty functions.

B. Chamber Characterization

The chamber characterization consists in a process where the target is to find a set of feasible working volumes considering high combined electric field and volume. This problem could be rewritten as an optimization problem as follows:

$$\begin{cases} \text{Max Working Volume} \\ \text{Max } \bar{\mathrm{E}}_{\mathrm{x,y,z}} \end{cases}$$
$$\text{S. t :}\mathbf{Max}(\hat{\sigma}_{\mathrm{x}}, \hat{\sigma}_{\mathrm{y}}, \hat{\sigma}_{\mathrm{z}}, \hat{\sigma}_{\mathrm{x,y,z}}) \leq \ 4 \text{ dB.} \tag{9}$$

The Pareto-set of this multiobjective problem was obtained by using the multiobjective genetic algorithm (MGA) [10].

C. Coupling the Field Computation Software and the Optimization Environment

The adopted procedure for both problems has three fundamental steps.

i) The field computation inside the reverberation chamber is performed using the FIT [11].
ii) The values of the electric field are exported to a file. The values are calculated over a regular grid.
iii) The working volume is calculated. For the determination of a particular working volume, (8) should be solved. The solution of (9) provides the characterization of the chamber.

At the final of step ii) a file is exported to our optimization environment.

The EMC standards adopt a parallelepiped as a working volume [2]. In this work we have adopted another solid to characterize the volume: an ellipsoid. This choice could be easily understood, due to computational aspects, (1) to (7) should be computed for every candidate volume. There is a set of sample points, i.e., the points of the regular grid and every point should be tested: If it is an inner point of the solid, it should be included on the computation. If this point is outside of the solid, then this point will be not included in the calculation. For computation purposes, the main advantage of using the ellipsoid is that, it needs only one comparison for determining if a point is inside or outside the ellipsoid. Taking into account a parallelepiped, it is necessary six comparisons, due to its six faces. Due to the stochastic nature of our optimization method, we have adopted an ellipsoid instead of a parallelepiped. Thus, both optimization problems (the mono-objective one and the multiobjective one) have six optimization variables: the two equatorial radii, the polar radius and three parameters associated to the ellipsoid translation (shift) from the chamber's centre. The physical constraints have been already described, but it can be also remarked that there is a very important geometric constraint: the working volume should be within the chamber. Therefore, the problem is bounded and the optimization variables are interconnected.

TABLE I
OPTIMIZATION VARIABLES

	Ellipsoid Axis			Shift of Chamber Centre		
	X	Y	Z	X	Y	Z
Minimum (m)	0	0	0	-2.6	-2.3	-1.35
Maximum (m)	2.6	2.3	1.35	2.6	2.3	1.35

TABLE II
WORKING VOLUME DETERMINATION

	X	Y	Z	Combined
Mean Electric Field (V/m)	0.73	1.16	1.10	1.0
Standard Deviation (dB)	3.79	3.61	3.48	3.96

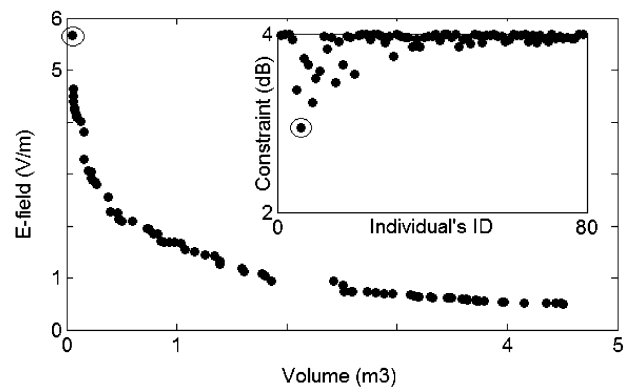

Fig. 2. Characterization of the chamber: the Pareto-set.

V. RESULTS

The Genetic Algorithm was applied to the working volume determination as proposed in [9]. A prescribed combined electric field equal to 1 V/m and a maximum value for the field homogeneity (4 dB) were used as constraints. Table I shows the range of the optimization variables.

The equality constraint plays a very important role in the optimization process. The solution of this problem is obtained at $[0.923\ 0.798\ 0.588\ -1.337\ 0.117\ 0.006]$. The first three values are the radii of the ellipsoid in the directions (x, y, z) and the last three values are the shifts from the centre of the chamber in the same direction. The working volume for this ellipsoid is 1.81 m^3. Table II shows some data concerning the physical behaviour of the working volume.

The same problem was also analyzed in order to characterize the chamber. The optimization problem described by (9) was solved by the methodology described in [10]. Fig. 2 shows the Pareto set, which correlates the combined electric field and the volume of the nondominated working volumes. The nondominated solutions of (9) should be feasible and Fig. 2 also shows, for each solution, the value of the maximum standard deviation (x, y, z or combined). It can be observed that the great majority of the solutions have very high electric field homogeneity. The majority of the solutions have the maximum standard deviation very close to the maximum prescribed one (4 dB).

In a multiobjective optimization problem, there are at least two points of view, when the solutions are achieved. Fig. 2 has shown the behaviour of the objective-functions and the constraint: for a maximal E-field, we have a minimal volume as

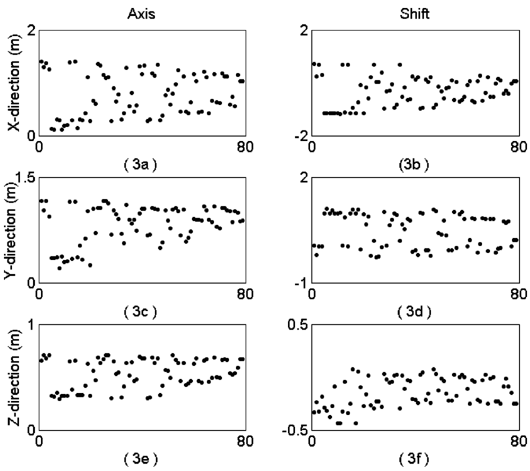

Fig. 3. Values of the optimization variables of nondominated solutions related to ellipsoid.

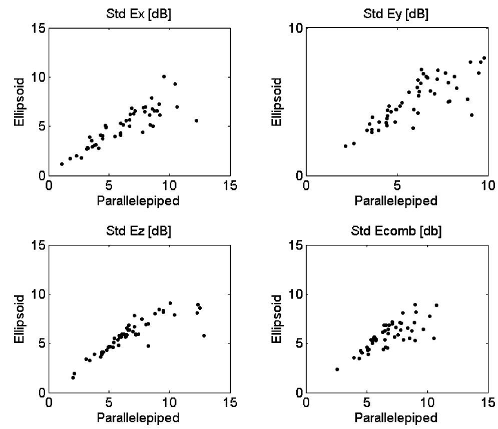

Fig. 4. Standard deviation for the parallelepiped and for the ellipsoid.

illustrated by the detached solution, in this case very far from border constraint.

Another interesting approach is to observe the values of the trends of optimization variables in the Pareto-set. Fig. 3 shows the six variables: three ellipsoid axes (x, y, z) and the three shifts of the centre of the ellipsoid. A positive shift value means that the centre of the working volume is close to the source wall. A negative shift of the working volume centre could be understood that the volume is close to the load. In a qualitative approach, we can observe in Fig. 3(e) and Fig. 3(f) that the lowest variance of the optimization parameters is associated to the axis in the z-direction and to the shift in the z-direction. This could be understood, due to the fact that the chamber minor dimension is the height (the z-direction). A good place to set up the EUT within this chamber is close to the middle height.

A. Effect of the Ellipsoid

Some questions could appear when an ellipsoid is used instead of a parallelepiped: what is the impact of this change on the accuracy of the working volume computation? The improvements in the values of electric field and in the standard deviation are high?

In order to interpret those questions a qualitative analysis was performed. We have generated a random set of feasible ellipsoid and for each ellipsoid it is possible to associate an external parallelepiped. The solids will be defined by the same set of parameters, i.e., the value of the shifts from the centre remains the same and the radii of the ellipsoid will become half of the size of the parallelepiped.

Fig. 4 shows the good correlation between the standard deviation values in x, y and z-directions and the combined one for the parallelepiped and for the ellipsoid. The great majority of the data have a correlation close to one. Nevertheless, there are some points that present low correlation. This could be understood due to the ratio of volumes between parallelepiped and the ellipsoid, which is close to two. In some cases, this difference is enough to produce a change in the analysis, because there is an underestimation of the standard deviation. The behaviour of the electric field is very similar to the ones shown in Fig. 4.

VI. Conclusion

The main goal of this work is to improve the characterization of reverberation chambers excited by transmission lines. GA and MGA features allow a large examination of its results. Based on all analyses and results in hand, the engineer can either choose any solution in the Pareto set, or restart the study considering different specifications and/or parameters. In that case, he will benefit from his better comprehension of the problem. While any discussion of electromagnetic compatibility is, by its very nature, complex, the presented work helps to better elucidate this important test environment.

Acknowledgment

This work was supported in part by the Brazilian foundations Capes, CNPq, and Fapesp.

References

[1] H. A. Mendes, A New Approach to Electromagnetic Field-Strength Measurements in Shield Enclosures Wescon, Tech. Papers, 1968, pp. 20–23.
[2] *Electromagnetic Compatibility (EMC), Part 4: Testing and Measurement Techniques—Section 21: Reverberation Chamber Test Methods*, IEC 61000-4, 2003.
[3] J. Perini and S. C. Lawrence, in *Proc. IEEE Int. Symp. Electromagn. Compat.*, 2000, pp. 633–637.
[4] T. Weiland, *Int. J. Numer. Mod.: ENDF*, vol. 9, pp. 259–319, 1996.
[5] D. Weinzierl, M. A. Santos, Jr., M. B. Perotoni, C. A. F. Sartori, J. R. Cardoso, and A. Kost, in *Proc. Int. Microwave Optoelectronics Conf.*, 2007, pp. 630–633.
[6] J. Clegg *et al., IEEE Trans. Electromagn. Compat.*, vol. 47, no. 4, pp. 824–832, 2005.
[7] P. Balling *et al.*, in *26th ESA Antenna Technology Workshop on Satellite*, 2003.
[8] C. A. Coello Coello, 2006 [Online]. Available: http://delta.cs.cinvestav.mx/~ccoello/EMOO/
[9] S. L. Avila, J. V. Leite, N. J. Batistela, J. P. A. Bastos, N. Sadowski, W. P. Carpes, Jr., and P. Kuo-Peng, *IEEE Trans. Magn.*, vol. 40, pp. 888–891, 2004.
[10] S. L. Avila, B. Sareni, and L. Krähenbuhl, in *9th Int. Workshop Optimization and Inverse Problems in Electromagnetism—OIPE*, Sorrento, 2006.
[11] [Online]. Available: http://www.cst.com/